Title: Mold-free fabrication of 3D microfeatures using laser-induced shock pressure

Authors: Balasubramanian Nagarajan, Sylvie Castagne, Zhongke Wang

PII: S0169-4332(13)00011-1
DOI: doi:10.1016/j.apsusc.2012.12.163
Reference: APSUSC 24923

To appear in: *APSUSC*

Received date: 10-10-2012
Revised date: 17-12-2012
Accepted date: 30-12-2012

Please cite this article as: B. Nagarajan, S. Castagne, Z. Wang, Mold-free fabrication of 3D microfeatures using laser-induced shock pressure, *Applied Surface Science* (2010), doi:10.1016/j.apsusc.2012.12.163

Mold-free fabrication of 3D microfeatures using laser-induced shock pressure

Balasubramanian Nagarajan[a,*], Sylvie Castagne[a], Zhongke Wang[b]

[a] SIMTech - NTU Joint Laboratory (Precision Engineering), School of Mechanical and Aerospace Engineering, Nanyang Technological University, 50 Nanyang Avenue, Singapore 639798

[b] Machining Technology Group, Singapore Institute of Manufacturing Technology, 71 Nanyang Drive, Singapore 638075

* Corresponding author:
Telephone : (65) 9861 2295
Fax : (65) 6792 4062
E-mail address : balasubr2@ntu.edu.sg
Postal address : SIMTech – NTU Joint Laboratory (Precision Engineering), School of Mechanical and Aerospace Engineering, Nanyang Technological University, N3-B4C-03, 50 Nanyang Avenue, Singapore 639798

Abstract

This paper reports on the fabrication of microfeatures on metallic foils using laser-induced shock forming without the assistance of micromold patterns. A mold-free laser shock forming technique, Flexible Pad Laser Shock Forming (FPLSF) has been developed and demonstrated to fabricate near-spherical microcraters on thin copper foils through the laser-generated plasma shock inducing plastic deformation on the copper foil. It is found that the crater formation strongly depends on the laser energy fluence applied to ablate an ablative overlay which is on top of the copper foil for plasma shock generation. Microfeatures with deformation depth of 80 μm to130 μm and radius of 485 μm to 616 μm were formed on 25 μm thick copper foils for the laser fluence of 7.3 J/cm^2 to 20 J/cm^2 while using aluminum foil as the ablative overlay and silicone rubber as a flexible support instead of a micromold. Fabrication of crater arrays on copper foils was also demonstrated successfully.

Keywords

Microforming, laser-induced shock loading, flexible-pad forming, thin metal foils

1. Introduction

The demand in manufacturing of microdevices used in various sectors including electronics, automobile, medical equipments, sensor technology and optics has been rapidly growing over the past decades. In general, the components of the microdevices or microsystems can be fabricated using several methods: lithographic techniques, micromachining, microforming, material deposition processes, etc. However, considering some process issues, such as limitations in the fabrication of high aspect ratio features, microtool fabrication, material compatibility, process flexibility, etc., it would be preferable to develop the fabrication methods which can compensate the process disadvantages.

Laser technology is one of the methods for the fabrication of microcomponents. So far, it has been used extensively in microcutting, microwelding, microforming, material deposition and surface patterning due to the localized laser beam control, process flexibility, and reliability [1]. In the recent years, fabrication of microfeatures on metal sheets using pulsed-laser driven deformation force has been accomplished [2-6]. A process for deforming 0.3 – 0.9 mm thick austenitic and ferritic stainless steel sheets using laser-induced shock waves has been demonstrated [7, 8]. Laser dynamic forming to deform metallic foils into a micromold with width ranging from 200 μm to 300 μm has been achieved, in which the geometry of the formed features on the foils was in conformance with that of the micromold [9]. Laser deep drawing is another technique developed by Vollertsen et al. to plastically deform 20 μm thick copper, aluminum and stainless steel sheets into spherical cups of 1 mm height using a TEA-CO_2 laser [3]. Very recently, microchannels with the dimension of 260 μm x 59 μm have been produced on 10 μm thick copper foils by laser shock embossing the copper foil on a micromold [5]. In spite of the differences in the reported processes above, the use of master micromold is necessary in all the processes for the fabrication of microfeatures on metal sheets or foils. It is well known that micromold fabrication is not only expensive but also limited in some complex microstructures, whereas the mold fabrication is achieved by Ultra-Precision Micromachining (UPM), micro-Electrical Discharge Machining (EDM), LIGA or laser ablation [10, 11]. Therefore, it is attractive to develop laser techniques which can produce microfeatures on

metal sheets or foils without the need of master micromold in the manufacturing of microdevices or microsystems.

In laser-induced shock forming processes, it has been noted that the geometry of the fabricated microfeatures is dependent not only on the micromold geometry but also on the laser process parameters such as the laser fluence, pulse duration, spot size, and the number of pulses [12, 13]. By varying the laser beam energy, different deformation depths of a microfeature have been achieved with the same micromold [2, 4, 14]. As the micromold is not the only factor to determine the microfeature geometry formed on metal sheets, it will be interesting to investigate the metal sheet deformation behavior under laser shock pressure using a flexible pad instead of using a micromold.

Therefore, this study focuses on developing a microfabrication technique to form microfeatures on metal foils using laser-generated plasma shock without the assistance from any specific master micromold patterns. Of particular interest is the study of microcrater formation on metal foils using the flexible pad laser shock forming (FPLSF), i.e. using pliable support as a flexible pad instead of using master mold pattern during the laser shock forming. Special effort has been made to determine the crater size dependence on the laser fluence applied to ablate the ablative overlay over the metal foil.

2. Experiments

The experimental setup of the FPLSF process is illustrated schematically in Fig. 1. A high-power pulsed laser is used to generate the shock pressure required for the metal foil deformation. The metal foil to be deformed is placed over a uniform flexible pad surface which is expected to play the role of master micromold. A hyperelastic polymer that can undergo large elastic deformation under loading is used as the flexible pad. The metal foil is covered with a uniform thin layer of an ablative overlay which absorbs the incident laser energy and generates plasma. It also acts as a thermo-protective layer to prevent the metal foil from thermal damages. A medium transparent to the laser beam is placed over the ablative overlay. This transparent medium is called confinement layer as it is used to restrict the plasma diffusion and direct the shockwave towards the foil surface. Due to the confinement layer, magnitude of the laser-induced shock pressure and the duration of shock wave are increased [15].

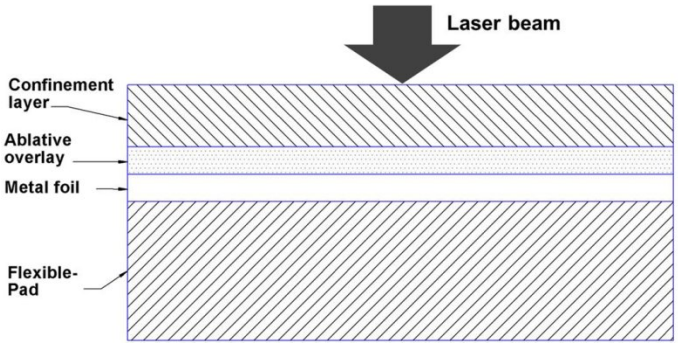

Figure 1. Schematic illustration of the setup of the flexible pad laser shock forming

In this study, annealed 99.9% pure copper foil of 25 μm thickness was used as the specimen. A Q-switched Nd:YAG laser which has a wavelength of 1.064 μm, pulse width of 38 ns, and maximum pulse energy of 75 mJ at 6 KHz was used for the laser irradiation. The laser beam has a squared energy profile with a focused size of 0.6 mm x 0.6 mm after a focal lens of 80 mm in focal length. For all experiments in this study, only one laser pulse was applied during the irradiation. Aluminum foil of 15 μm in thickness was used as the ablative overlay due to its small vaporization threshold. More importantly, aluminum foil can be peeled off easily from the deformed foil surface after the completion of the laser shock forming, unlike other ablative materials such as paint coating and black tape which are hard to remove from the foil surface. A thin layer of vacuum grease was applied between the ablative overlay and the copper foil in order to provide an accurate sealing. Deionized water was used as the confinement layer. The entire setup was placed in a container with water filled up to 4.2 mm above the copper foil. Silicone rubber of 0.3 mm thickness was used as the flexible pad against which the sheet deformation occurs.

According to the critical thickness (e_m) of the confinement layer, $e_m = 0.5\tau D$, where τ is the laser pulse duration and D is the shock velocity, the minimum thickness of the water layer required was calculated to be 31.35 μm at τ of 38 ns and D of 1650 ms^{-1} [16]. However, when the confinement thickness of water layer was smaller than 3 mm, damage of copper surface under the laser shock was observed in our study. On the other hand, when the confinement water layer was too thick, it led to a significant reduction in the laser intensity due to the strong absorption of the water to the laser energy. Thus, the optimum thickness of 4.2 mm was used in this experiment. The thickness of the rubber pad should be at least 1.5 to 2 times greater than the depth of the forming cup in the rubber pad forming process [17]. The maximum depth

of craters was measured to be about 150 μm in our FPLSF experiments. Thus, a silicone rubber with a thickness of 300 μm which was the double of the maximum crater depth was used.

Talyscan 3D surface profiler was used to measure the deformation geometry and the surface topographies. Bottom surface of the crater was scanned by a stylus probe (diamond tip with a radius of 2 μm) rather than the top surface due to the limitations of scanning the samples at the top surface. Scanning electron microscope (SEM) was used to observe the surface of the craters formed in copper foil and the ablation of the aluminum foil overlay after the irradiation.

3. Results and discussions

3.1. Generation of craters

Experiments were conducted initially to investigate the feasibility of FPLSF for fabricating micro-deformation craters in copper foils with a laser fluence of 13.6 J/cm^2. Figures 2a and 2b show the SEM image of the top and bottom surface of the formed crater for a single-pulse irradiation respectively. Figures 2c and 2d show the 3D topography and the cross-section at the center of the crater measured at its bottom surface. In this study, the deformation depth and diameter of the formed sample are characterized by the bulge height (h) and bulge diameter (D_b) as indicated in Fig. 2e. The bulge height (h) and the crater depth (d) are related to the difference in copper foil thickness ($\Delta t = h - d$) before and after FPLSF.

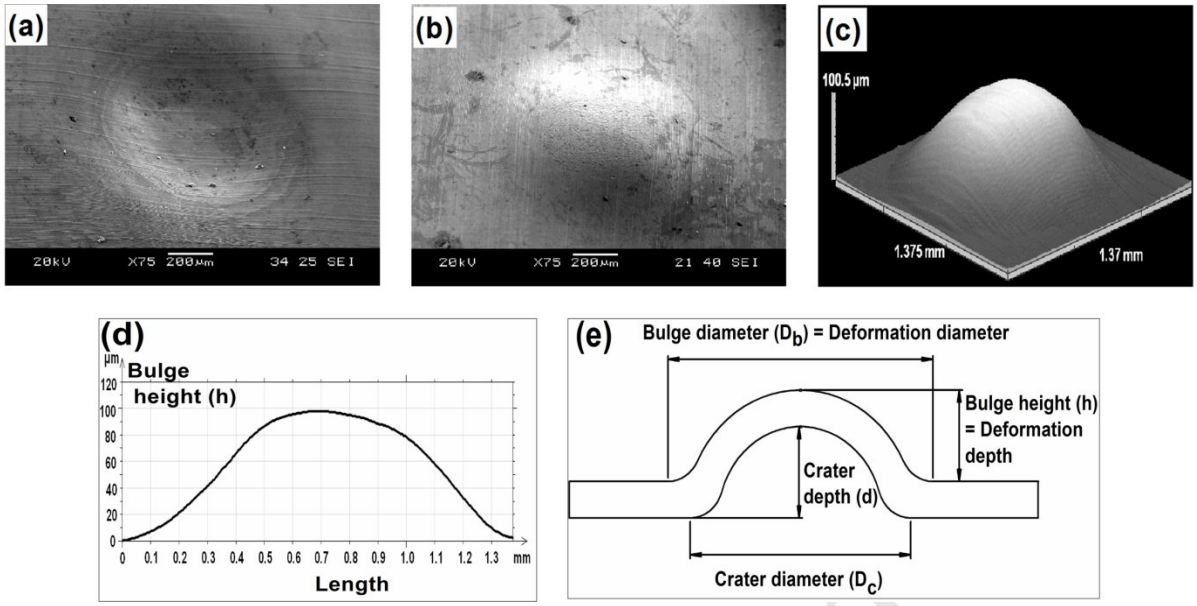

Figure 2. Crater formation on copper foil through FPLSF under the laser fluence of 13.6 J/cm^2. (a) SEM image of the top surface of the crater (b) SEM image of the bottom surface of the crater; Crater profiles measured by the stylus profilometer at the bottom surface (c) 3D topography of the crater (d) Cross-sectional profile of the crater (e) Method to measure the deformation depth and diameter of the formed sample

The deformation depth (h) of the formed sample for the laser fluence of 13.6 J/cm^2 is 95.6 µm. Maximum deformation depth was observed at the center of the crater. The deformation force that is exerted on the metal foil which is placed over the silicone rubber depends upon the laser-induced shock loading. The peak laser-induced shock pressure P according to Fabbro's model [15] is given as follows:

$$P\,(\mathrm{GPa}) = 0.01\sqrt{\frac{\alpha}{3+2\alpha}}\sqrt{I_0\,(\mathrm{GW/cm^2})\;Z\,(\mathrm{g/cm^2 s})} \qquad (1)$$

where α is the fraction of internal energy used to increase the plasma thermal energy, I_0 is the laser intensity and Z is the shock impedance that is calculated by $2/Z = 1/Z_1 + 1/Z_2$, in which Z_1 and Z_2 are shock impedances of target and confinement materials respectively. The peak shock pressure calculated from Fabbro's model for 13.6 J/cm^2 laser fluence is 0.58 GPa whereas α = 0.1, Z_1 (Aluminum) = 1.5 x 10^6 g cm^{-2} s^{-1} and Z_2 (Water) = 0.165 x 10^6 g cm^{-2} s^{-1} [18].

The deformation diameter (D_b) of the formed sample was 1.3 mm as shown in Fig. 2d which is greater than the square beam of 0.6 mm side. This behavior can be attributed to the high thermal energy of the laser radiation which vaporizes the ablative overlay of area larger than the ideal irradiation area. It is also observed from Fig. 2 that the shape of the deformation crater was hemi-spherical even though the beam profile was square-shaped. This behavior of

hemispherical crater formation can be attributed to the spherically propagating shockwave from the top surface of the copper foil upon irradiation [19].

Silicone rubber retracted to its initial position once the deformed metal foil is removed from the rubber surface. No occurrence of rubber failure was observed after using the same rubber for several experiments as it was subjected only to small number of loading cycles in this study. However, the rubber pad may get damaged after large number of loading cycles.

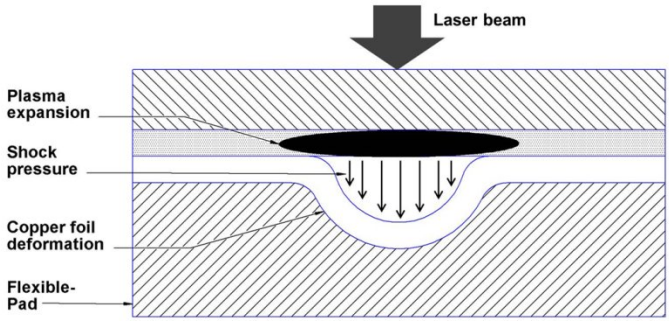

Figure 3. Crater formation mechanism on a metal foil through FPLSF

The deformation mechanism of FPLSF is illustrated in Fig. 3. During irradiation, the laser beam travels through the confinement layer and vaporizes the top portion of the ablative overlay material into a high pressure and high temperature plasma instantaneously. The produced plasma expands in the confined space between the workpiece and confinement layer and induces shockwaves that are propagating into the metal foil and the confinement [15]. The shockwave directed towards the workpiece transfers the momentum to the foil and induces plastic deformation when the induced shock pressure is greater than the dynamic yield strength of the material. During the shock loading, the flexible pad undergoes large elastic deformation along with the plastic deformation of metal foil. The flexible pad retracts to its original position once the metal foil is removed from the pad whereas a permanent deformation is induced on the metal foil. The replacement of micromold with the flexible pad in FPLSF provides following significant advantages to the deformation behavior of metal foil: (i) While deforming metal foils using micromolds, fracture of material occurs in the mold fillet region where the local plastic strains are high [4]. As a flat flexible pad is used in this process, the possibility of stress localization will be reduced thereby minimizing the occurrence of foil fracture. (ii) If the forming velocity of the metal foil is higher than a critical velocity, fracture of material takes place [13]. For processes with the micromolds, the forming velocity of the

material may reach the critical velocity as the deformation is not restricted until it reaches the mold bottom. In FPLSF, as the deformation of the metal foil is controlled by the stiffness of the flexible pad, forming velocity of the metal foil is controlled and the occurrence of fracture will be reduced.

3.2. Influence of laser fluence on crater profile

Though the feasibility of FPLSF to induce plastic deformation on thin copper foils has been demonstrated, the capability of FPLSF to produce different deformation crater geometry has to be tested. It is known from the literature that the laser pulse energy is one of the significant process parameters that influences the deformation profile in laser shock forming processes with mold [4, 7, 8]. Therefore, experiments were performed to analyze the effect of laser fluence on copper deformation in FPLSF with laser fluence values ranging from 1 J/cm^2 to 21 J/cm^2. Three samples were tested at each laser fluence value and the average deformation depth (h), deformation diameter (D_b) and the aspect ratio (D_b/h) of the samples are illustrated in Fig. 4.

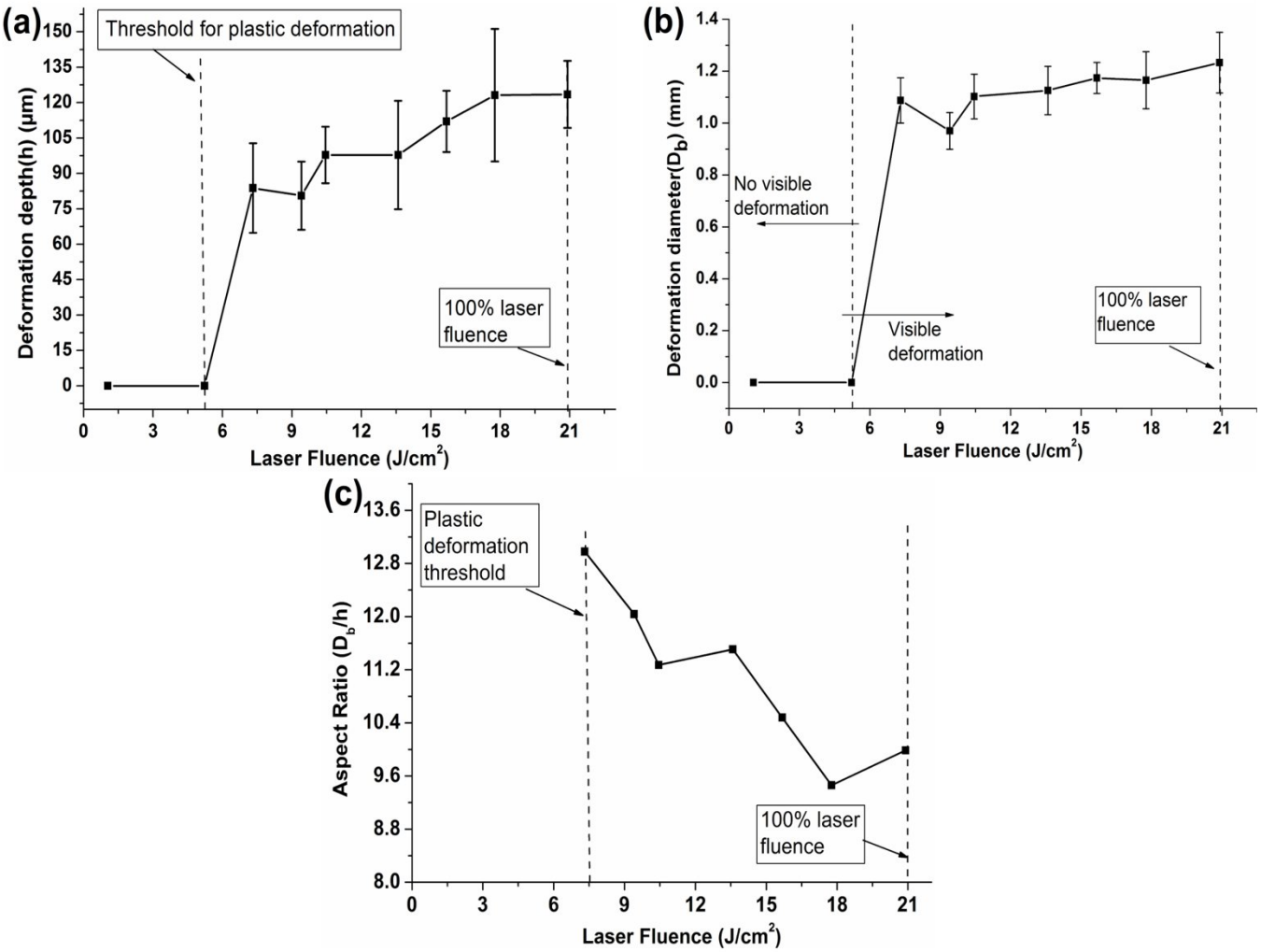

Figure 4**.** Influence of laser fluence on the geometry of craters formed on copper foil (a) Deformation depth (h) (b) Deformation diameter (D_b) (c) Aspect ratio (D_b/h)

Experimental results as shown in Fig. 4 illustrate that copper foil experienced no plastic deformation until a certain threshold of laser fluence (5.2 J/cm^2) is exceeded. Until this threshold, laser fluence was insufficient to induce the shockwave pressure (peak pressure is 0.42 GPa for 5.2 J/cm^2 according to Fabbro's model) greater than the dynamic yield strength of copper. For laser fluence below the threshold, two different behaviors related to the ablation of the ablative overlay can be responsible for the absence of plastic deformation of copper: (i) Laser energy is insufficient to vaporize the aluminum foil so that no plasma and shockwave formation are experienced. (ii) Ablation of aluminum foil is limited to small thickness at the top portion. Thus, the propagating shockwave is attenuated by the remaining thickness of the aluminum foil. Once the threshold is exceeded, the deformation depth increased along with the

laser fluence. According to Fabbro's model, the plasma-induced shock pressure is dependent on the laser intensity [15]. Therefore, the increase in depth can be attributed to the increase in shock pressure exerted on the metal foil.

Similarly, increase in deformation diameter (D_b) was observed along with the laser fluence (Fig. 4b). The minimum deformation diameter obtained was approximately 1 mm for the lowest laser fluence that induced deformation. For increase in laser fluence, shockwave amplitude is higher and also the heat conduction extends to a larger area in the aluminum foil. This behavior increases the aluminum vaporization zone and hence the deformation diameter. It is observed from Fig. 4 that the maximum deformation depth and diameter were obtained for 20.9 J/cm^2 fluence which is the maximum laser output energy, i.e. 100% laser fluence. A minor deviation of deformation diameter from the increasing trend was observed at 9.4 J/cm^2 fluence. This behavior can be attributed to the unstable first laser pulse and the non-uniform vacuum grease thickness. However, while considering the standard deviation of the diameter values, the increasing tendency of the average deformation diameter can be still observed.

It is observed from Fig. 4c that the aspect ratio of the craters reduced with the increase in laser fluence. Comparing Fig. 4 and Fig. 5, it can be found that the increase in depth (h) was greater than the increase in diameter (D_b) for the increase in laser fluence.

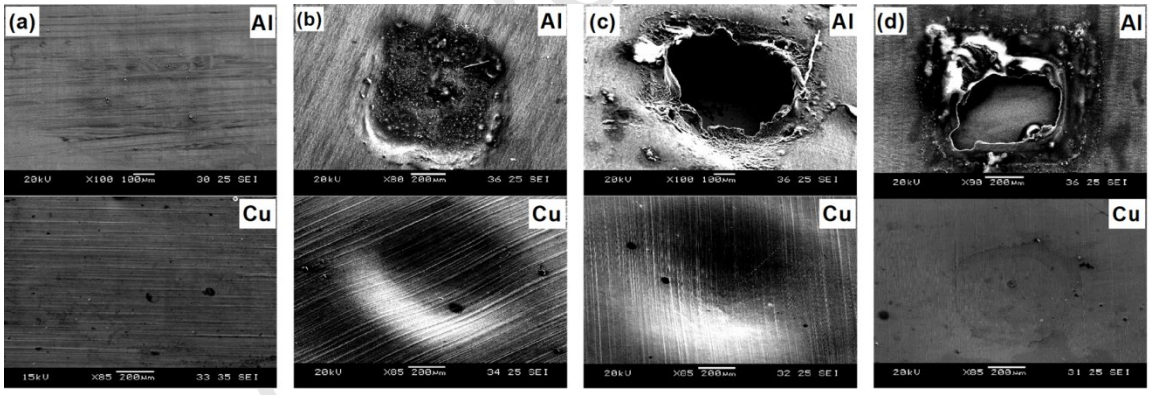

Figure 5. Influence of aluminum foil ablation on crater formation in copper foil for different laser fluence (a) No ablation of aluminum foil and no crater formation in copper foil at 5.2 J/cm^2 (b) Partial ablation of aluminum foil followed by the crater formation on copper foil at 7.3 J/cm^2 (c) Ablation of entire thickness of aluminum foil and the crater formation at 20.9 J/cm^2 laser fluence (d) Damage of copper surface at 20.9 J/cm^2 laser fluence with ablation of entire thickness of aluminum foil

The difference in ablation behavior of aluminum foil for the change in laser fluence is illustrated in Fig. 5. At 5.2 J/cm^2 fluence which is the fluence threshold, no ablation of aluminum foil was observed as shown in Fig. 5a. Correspondingly, no crater was formed on the copper foil at 5.2 J/cm^2 fluence (Fig. 5a). Above the fluence threshold, only the top portion of aluminum foil was ablated at 7.3 J/cm^2 as shown in Fig. 5b. This partial ablation of ablative overlay is the reason for the formation of crater with no thermal damage to the copper surface at the 7.3 J/cm^2 fluence (Fig. 5b). For higher laser fluence (20.9 J/cm^2), the entire thickness of the aluminum foil was ablated which is shown in Fig. 5c. It is interesting to observe from Fig. 5c that the craters were formed on copper foil with no significant thermal damage at 20.9 J/cm^2 fluence though the entire thickness of aluminum foil was ablated. This damage-free copper surface at 20.9 J/cm^2 could be attributed to the following factors: (a) High reflectivity of copper at 1064 nm wavelength may reduce the absorption of laser by copper surface and any possible melting, (b) any possible melt debris of aluminum foil on the copper surface will be solidified instantaneously as the melting point of aluminum (660.4°C) is lesser that the melting point of copper (1085°C), (c) vacuum grease which is existing between the copper and aluminum foils prevents the aluminum debris to contact the copper surface and also vaporized upon interaction with the laser. However,minor damages on the copper surface was observed for the laser fluence of 20.9 J/cm^2 at some instances as shown in Fig 5d. Therefore, it is understood that the ablation of aluminum foil has a significant effect in FPLSF to produce damage-free surface of the crater.

3.3. Fabrication of crater arrays

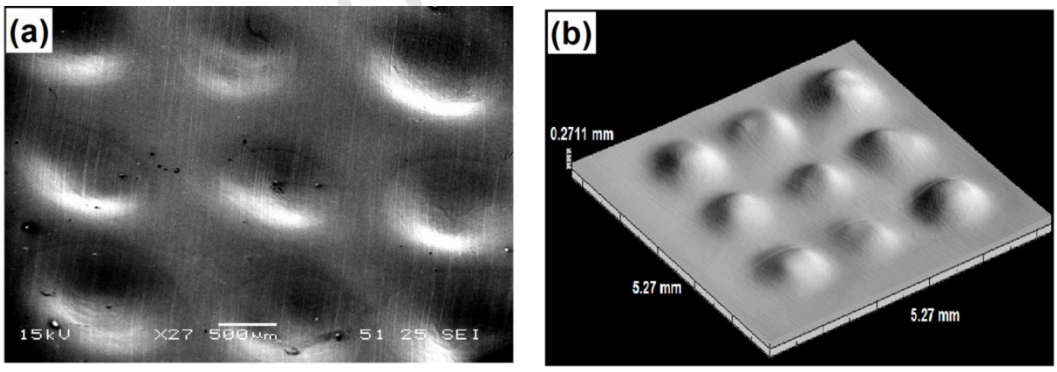

Figure 6. Crater arrays for the laser fluence of 7.3 J/cm^2 (a) SEM image (30^0 tilt) of the irradiated side of the craters (b) Topography of the formed craters measured from the bottom surface

An array of craters was produced on copper foils as shown in Fig. 6 to demonstrate the reproducibility of FPLSF. Smallest laser fluence of 7.3 J/cm^2 for which deformation is minimum and pitch length of 1.5 mm were used to fabricate the craters in the 3x3 array. It is observed that the formed craters were uniform in shape and size which highlights the controllability of FPLSF process to produce uniform microfeatures on thin metal sheets. As the crater diameter was greater than 1 mm, the pitch length of 1.5 mm was used between the array craters to avoid the interference of shockwaves propagating from adjacent irradiation spots. By reducing the beam sizes, generation of crater arrays with narrow pitch length is feasible due to the reduction of individual crater diameter. A small deviation between the formed craters was observed which can be attributed to the instability of the first pulse, minor variation in focus and the non-uniform thickness of the vacuum grease applied between copper foil and the ablative overlay.

4. Conclusion

This paper demonstrated the Flexible-Pad Laser Shock Forming (FPLSF) process which is a mold-free microforming technique using the laser-induced shockwaves and a flexible pad to induce plastic deformation on metal foils. Using FPLSF, microcraters of depth ranging between 80 μm and 130 μm and radius ranging between 485 μm and 616 μm were formed on copper foils of 25 μm thickness for the laser fluence varying between 7.3 J/cm^2 and 20 J/cm^2. It was observed that the formed craters were in hemi-spherical shape though the laser beam was square-shaped. The deformation depth and diameter of the craters depended upon the laser fluence parameter. Hence, it is understood that, various deformation crater profiles can be achieved using FPLSF by controlling the laser processing parameters with the help of a flexible pad. However, it could be possible to produce different feature shapes by controlling the shape and intensity of the beam, and the sample motion during the energy loading. Nevertheless, FPLSF is not able to fabricate different feature shapes as intricate as the feature shapes produced by the processes using micromold. FPLSF possesses the following significant advantages:

- The process has high flexibility as the same backing pad can be used to fabricate different features by controlling the laser beam size and fluence.
- Short process cycle time due to nanosecond laser pulses and the ease of alignment. As no damage to the flexible backing is observed after shock pressure application, it can be reused for large number of cycles.

Acknowledgement

This work is supported by Machining Technology Group, Singapore Institute of Manufacturing Technology under CRP Project Number U11-M-013U.

References

[1] A. Gillner, J. Holtkamp, C. Hartmann, A. Olowinsky, J. Gedicke, K. Klages, L. Bosse, A. Bayer, Laser applications in microtechnology, J. Mater. Process. Technol., 167 (2005) 494-498.

[2] J.Z. Zhou, J.C. Yang, Y.K. Zhang, M. Zhou, A study on super-speed forming of metal sheet by laser shock waves, J. Mater. Process. Technol., 129 (2002) 241-244.

[3] F. Vollertsen, H. Niehoff, H. Wielage, On the acting pressure in laser deep drawing, Prod. Eng., 3 (2009) 1-8.

[4] H. Gao, C. Ye, G.J. Cheng, Deformation Behaviors and Critical Parameters in Microscale Laser Dynamic Forming, J. Manuf. Sci. Eng.-Trans. ASME, 131 (2009) 051011.

[5] H. Liu, Z. Shen, X. Wang, H. Wang, M. Tao, Micromould based laser shock embossing of thin metal sheets for MEMS applications, Appl. Surf. Sci., 256 (2010) 4687-4691.

[6] H. Liu, Z. Shen, X. Wang, H. Wang, Numerical simulation and experimentation of a novel laser indirect shock forming, J. Appl. Phys., 106 (2009) 063107.

[7] M. Zhou, Y.K. Zhang, L. Cai, Ultrahigh-strain-rate plastic deformation of a stainless-steel sheet with TiN coatings driven by laser shock waves, Appl. Phys. A-Mater. Sci. Process., 77 (2003) 549-554.

[8] M. Zhou, Y. Zhang, L. Cai, Laser shock forming on coated metal sheets characterized by ultrahigh-strain-rate plastic deformation, J. Appl. Phys., 91 (2002) 5501-5503.

[9] G.J. Cheng, D. Pirzada, Z. Ming, Microstructure and mechanical property characterizations of metal foil after microscale laser dynamic forming, J. Appl. Phys., 101 (2007) 063108-063107.

[10] Y. Qin, A. Brockett, Y. Ma, A. Razali, J. Zhao, C. Harrison, W. Pan, X. Dai, D. Loziak, Micro-manufacturing: research, technology outcomes and development issues, Int. J. Adv. Manuf. Technol., 47 (2010) 821-837.

[11] J. Fleischer, J. Kotschenreuther, The manufacturing of micro molds by conventional and energy-assisted processes, Int. J. Adv. Manuf. Technol., 33 (2007) 75-85.

[12] R. Fabbro, P. Peyre, L. Berthe, X. Scherpereel, Physics and applications of laser-shock processing, J. Laser Appl., 10 (1998) 265-279.

[13] J. Li, G.J. Cheng, Multiple-pulse laser dynamic forming of metallic thin films for microscale three dimensional shapes, J. Appl. Phys., 108 (2010) 013107-013108.

[14] H. Niehoff, F. Vollertsen, Laser induced shock waves in deformation processing, METALURGIJA - Journal of Metallurgy, 11 (2005) 183.

[15] R. Fabbro, J. Fournier, P. Ballard, D. Devaux, J. Virmont, Physical study of laser-produced plasma in confined geometry, J. Appl. Phys., 68 (1990) 775-784.

[16] J.P. Romain, P. Darquey, Shock waves and acceleration of thin foils by laser pulses in confined plasma interaction, J. Appl. Phys., 68 (1990) 1926-1928.

[17] M. Ramezani, Z. Ripin, Analysis of deep drawing of sheet metal using the Marform process, Int. J. Adv. Manuf. Technol., 59 (2012) 491-505.

[18] D. Devaux, R. Fabbro, L. Tollier, E. Bartnicki, Generation of shock waves by laser-induced plasma in confined geometry, J. Appl. Phys., 74 (1993) 2268-2273.

[19] Y. Hu, Z. Yao, J. Hu, 3-D FEM simulation of laser shock processing, Surf. Coat. Technol., 201 (2006) 1426-1435.

Highlights

- A new microfabrication technique for the formation of microfeatures on metal foils without the micromolds is proposed.
- Forming of craters on copper foils achieved using a flexible-pad and laser-induced plasma shock pressure.
- Different microfeature sizes are obtained by varying the laser fluence.
- Short process cycle time and improved flexibility due to the elimination of micromolds in microforming.